Insect Biochemistry and Molecular Biology 156 (2023) 103935

Contents lists available at ScienceDirect

Insect Biochemistry and Molecular Biology

journal homepage: www.elsevier.com/locate/ibmb

Diverse functions of the ecdysone receptor (EcR) in the panoistic ovary of the German cockroach

M. Rumbo, V. Pagone, M.D. Piulachs *

Institut de Biologia Evolutiva (CSIC- Universitat Pompeu Fabra), Passeig Maritim de la Barceloneta, 37, 08003, Barcelona, Spain

ARTICLE INFO

Keywords:
Blattella germanica
Ecdysone
Ecdysteroidogenic genes
Insect oogenesis
Panoistic ovary

ABSTRACT

Ecdysone regulates essential processes in insect life. Perhaps the most well-known of these are related to metamorphosis. However, ecdysone is also required to regulate the proliferation and differentiation of germ cells in the ovary. The role of ecdysone in insect oogenesis has been studied in depth in holometabolan species with meroistic ovaries, such as *Drosophila melanogaster*, while in hemimetabolan species with panoistic ovaries their functions are still poorly understood. In the present work, we studied the role of ecdysone in the ovary of the last nymphal instar of the cockroach *Blattella germanica* by using RNA interference to reduce the levels of the ecdysone receptor (*EcR*), and thereby deplete the expression of ecdysteroidogenic genes in the prothoracic gland. However, the expression of ecdysteroidogenic genes was upregulated in the ovary, resulting in cell over-proliferation in the germarium, which appeared swollen. By analysing the expression of genes that respond to ecdysone, we found that when the source of 20E is the nymphal ovary, *EcR* appears to repress 20E-associated genes bypassing early genes signalling.

1. Introduction

The steroid hormone ecdysone is known for its crucial role in the control of several developmental processes in the life cycle of insects, especially regarding moulting and metamorphosis. In addition, it is also a key player in female reproductive physiology, as it is essential for oocyte maturation, oocyte survival, and fertility, among other processes (Finger et al., 2021). During the juvenile stages, ecdysone is synthesized by the prothoracic gland (King et al., 1974; Nation, 2008; Romañá et al., 1995). However, this gland degenerate when the insects reach adulthood, then the ovaries become main source of ecdysone (Klowden, 2007; Pascual et al., 1992; Romañá et al., 1995).

In adult insects, the role of ecdysone has been described in relation to oocyte maturation, especially from vitellogenesis to choriogenesis. Moreover, this role has been mainly studied in insects with meroistic ovaries, such as the fruit fly *Drosophila melanogaster* (see Bellés and Piulachs, 2015) or the silkworm *Bombyx mori* (see Swevers and Iatrou, 2009). Conversely, the roles of ecdysone in the early stages of oogenesis have been poorly studied. During the adult stage of *D. melanogaster*, ecdysone is mainly synthetized by the ovarian somatic cells. In these cells, ecdysone and the biologically more active metabolite 20-hydroxyecdysone (20E), regulate several processes, such as cell proliferation, maintenance and differentiation of germinal stem cells, border cell migration, egg chamber formation, control of mid-late oogenesis, choriogenesis and ovulation (Swevers, 2019).

The function of ecdysone in oogenesis in other insect species may differ, depending on the ovariole type or factors associated with oocyte growth, such as blood feeding or the transfer of ecdysteroids by males during mating, as occurs in the mosquito *Anopheles gambiae* (Baldini et al., 2013; Robinson, 2013). In the red flour beetle *Tribolium castaneum*, and in the kissing bug *Rhodnius prolixus*, both species with meroistic telotrophic ovaries, 20E signaling impairment achieved by depleting *shade* (*shd*), *ecdysone receptor* (*EcR*) or *ultraspiracle* (*usp*) expression, blocks ovarian growth and maturation of the basal follicle, accompanied by defects in the migration of follicle cells (Benrabaa et al., 2022; Parthasarathy et al., 2010).

The information available about the function of 20E in panoistic ovaries is scarce. Administration of exogenous 20E in adult females of the cricket *Gryllus bimaculatus* increases the total number of eggs oviposited, and accelerates ovarian maturation (Behrens and Hoffmann, 1983). In the desert locust *Schistocerca gregaria*, depletion of *EcR* expression determines changes in ovarian maturation, and prevents chorion formation and oviposition (Lenaerts et al., 2019). In the Pacific beetle cockroach, *Diploptera punctata*, *EcR* and *usp* mediate oviposition

* Corresponding author.
E-mail address: mdolors.piulachs@ibe.upf-csic.es (M.D. Piulachs).

https://doi.org/10.1016/j.ibmb.2023.103935
Received 18 November 2022; Received in revised form 23 March 2023; Accepted 23 March 2023
Available online 28 March 2023

and choriogenesis, but are not involved in oocyte growth (Hult et al., 2015). The action of 20E in the German cockroach, *Blattella germanica*, has been reported in relation to choriogenesis (Bellés et al., 1993; Pascual et al., 1992), while more recently, we described that 20E administered to newly emerged last instar *B. germanica* nymphs led to an increase in the number of differentiated ovarian follicles in the ovariole (Ramos et al., 2020).

In the present work, we used RNA interference (RNAi) to deplete the expression of *EcR*, the 20E receptor, in order to study the effect of impairing 20E signalling on the oogenesis of *B. germanica*. Among other possible effects, we expected to obtain the opposite phenotype to that observed when administering 20E. Thus, we presumed that the combination of the results of both conditions would help us define the still obscure role of 20E in *B. germanica* oogenesis. In turn, we hoped that this would allow us to assess whether the ecdysone signalling pathway associated with oogenesis has been conserved in the evolutionary transition from panoistic to meroistic ovaries, or whether this transition involves new regulatory changes. Here we focused on the sixth (last) nymphal instar because the final number of ovarian follicles in the ovariole is established during this instar in *B. germanica* (Ramos et al., 2020).

A single isoform of *EcR*, known as *EcR*-A, has been reported in *B. germanica* in the context of a study of the effects of *EcR* depletion on the imaginal molt (Cruz et al., 2006). Moreover, *EcR* depletion impairs ecdysone synthesis in the prothoracic gland because ecdysteroid levels in the haemolymph are reduced (Cruz et al., 2006). In addition, two different effects in the ovaries of nymph and adult *B. germanica* were reported: *EcR* depletion led to a reduction of follicular cell proliferation in the basal ovarian follicle in nymphs, and to an impairment of choriogenesis in the adult (Cruz et al., 2006).

In this work, we report that the expression of ecdysteroidogenic genes in the prothoracic gland is reduced after *EcR* depletion. We showed that *EcR* can function as a repressor of ecdysone-dependent genes in the prothoracic gland or activator of them in the ovaries. We also found out that transduction of the ecdysone signal by *EcR* in nymphal ovaries can follow different pathways, depending on the origin of 20E. *EcR* can transduce the hormonal signal through the canonical ecdysone cascade (Ashburner, 1980) if the ecdysone comes from the prothoracic gland through the haemolymph. However, when ecdysone is synthesized by the ovary itself, *EcR* can act directly on genes downstream of the ecdysone cascade.

2. Material and methods

2.1. Cockroach colony and tissue sampling

Nymphs and adults of *B. germanica* were obtained from a colony fed ad libitum on Panlab 125 dog chow and water and reared in the dark at 29 ± 1 °C and 60–70% relative humidity. All dissections and tissue samplings were performed on carbon dioxide-anaesthetized specimens.

2.2. RNAi experiments

To deplete the expression of *EcR*, a dsRNA (ds*EcR*) was designed targeting the ligand binding domain (LBD) of *EcR* (570 bp) (Cruz et al., 2006). A dsRNA corresponding to 307 bp of the *Autographa californica* nucleopolyhedrovirus sequence (dsPolyH) was used as a control. The dsRNA was synthesized in vitro using the kit MEGAscript RNAi (Thermo Fisher Scientific, Carlsbad CA, USA) and the dsRNA obtained was purified with phenol: chloroform: isoamyl alcohol (25:24:1). Freshly emerged last-instar female nymphs (N6D0) and newly emerged adult females, were treated with 1 μg of either dsEcR or dsPolyH injecting 1 μL of this solution into the abdomen with a Hamilton microsyringe. We will refer to the RNAi treatments as ds*EcR* and dsPolyH. The sequences of the primers used are listed in Table S1.

2.3. RNA extraction and expression studies

Dissections of prothoracic gland were performed on 6-day-old sixth instar nymph (N6D6) females. Dissections of ovaries were performed on N6D6 and in 7-day-old adults. Samples were frozen with liquid nitrogen, and total RNA was isolated from dissected organs using the HigherPurity™ Tissue Total RNA Purification kit (Canvax Biotech S.L., Córdoba, Spain). Quantification and quality analysis of total RNA was obtained by spectrophotometric absorption at 260/280 nm in a Nabi UV/Bis Nano Spectrophotometer (MicroDigital Co, Ltd). A total of 150 ng of the extracted RNA from each ovary sample was DNAse treated (Promega, Madison, WI, USA), and reverse transcribed with Transcriptor First Strand cDNA Synthesis Kit (Roche LifeScience). For prothoracic gland, the total amount of RNA extracted was reverse transcribed.

The expression levels of genes under study were determined by quantitative real time PCR (qRT-PCR). PCR primers used in qRT-PCR expression studies were designed using the Primer3 v.0.4.0 (Rozen and Skaletsky, 2000). qRT-PCR reactions were made using the iTaq Universal SYBR Green Supermix (BioRad) containing 200 nM of each specific primer (performed in triplicate). Amplification reactions were carried out at 95 °C for 2 min, and 40 cycles of 95 °C for 15 s and 60 °C for 30 s, using MyIQ Single Color RTPCR Detection System (BioRad). After the amplification phase, levels of mRNA were calculated relative to the housekeeping gene *actin-5c* using the $2^{-\Delta\Delta Ct}$ method (Irles et al., 2009; Livak and Schmittgen, 2001; Maestro et al., 2005). Results are given as copies of mRNA per 1000 copies of *actin-5c* mRNA (Irles et al., 2009). The sequence of the primers used in the work, and the accession number of genes analyzed are detailed in Table S1.

2.4. Immunohistochemistry

Ovaries from N6D6 (24 ds*PolyH* and 19 dsEcR females) were dissected and immediately fixed in paraformaldehyde (4% in PBS) for 1h. Washing samples and antibody incubations were performed as previously described (Irles and Piulachs, 2014). The primary antibodies employed were mouse anti-EcR (10F1) dilution 1:50, obtained from the Developmental Studies Hybridoma Bank. (Department of Biology, University of Iowa, Iowa City, IA). The secondary antibody used was goat anti-mouse IgG conjugated with Alexa Fluor 647 (Molecular Probes, Carslbad, CA). Next, ovaries were incubated at room temperature for 20 min in 300 ng/mL phalloidin-TRITC (Sigma) and then for 5 min in 1 μg/mL DAPI (Sigma) PBT, to stain F-actin and nuclei, respectively. After three washes with PBT, ovaries were mounted in Mowiol (Calbiochem, Madison, WI, USA) and observed using Zeiss AxioImager Z1 microscope (Apotome) (Carl Zeiss MicroImaging). We considered that an ovarian follicle has been released from the germarium when the follicular epithelium surrounding the oocyte is identifiable.

To name these different cell types identified in *B. germanica* germarium, we take as a reference the meroistic ovary from *D. melanogaster*, which has been thoroughly described (see Drummond-Barbosa, 2019; Hayashi et al., 2020; Hsu et al., 2019, for example), as well as the descriptions reported in the panoistic ovaries of *Thermobia domestica*, *Bacillus rossius* and *Parthenothrips dracenae* (Pritsch and Büning, 1989; Taddei et al., 1992; Tworzydlo et al., 2014).

2.5. Statistics

The data are expressed as mean ± standard error of the mean (S.E.M.). Statistical analyses were performed using GraphPad Prism version 8.1.0 for Windows, GraphPad Software (San Diego, California, USA). The significance of the gene expression differences, between control and treated groups, were calculated using the Student's *t*-test.

3. Results

3.1. EcR expression in Blattella germanica ovaries

EcR is expressed in the ovaries throughout the entire gonadotrophic cycle (Fig. 1A), with some fluctuations that do not generally correlate with the ecdysone profile, neither in the ovary nor circulating in the haemolymph. In the adult ovary a significant increase in *EcR* expression is observed at day 4 ($p = 0.02$ compared to expression on day 3), which coincides with the increase of ovarian ecdysteroid levels (Romañá et al., 1995) and the arrest of cytokinesis in the follicular cells of the basal ovarian follicle, that become binucleated (Büning, 1994). Maximal expression is observed at the end of the cycle, just before oviposition, overlapping with choriogenesis, and the highest levels of ovarian ecdysone (Fig. 1A). Using immunolabelling, EcR protein can be detected in all ovarian follicles in the vitellarium of sixth (last) instar nymphs (Fig. 1B), the labelling intensity decreasing as oocyte maturation progresses (Fig. 1B and C). EcR labelling can be detected in both the oocytes and in the follicular cells. In the oocytes it appears in the cytoplasm and in the nucleus, accumulating at the nuclear membrane in all differentiated oocytes (Fig. 1B–D).

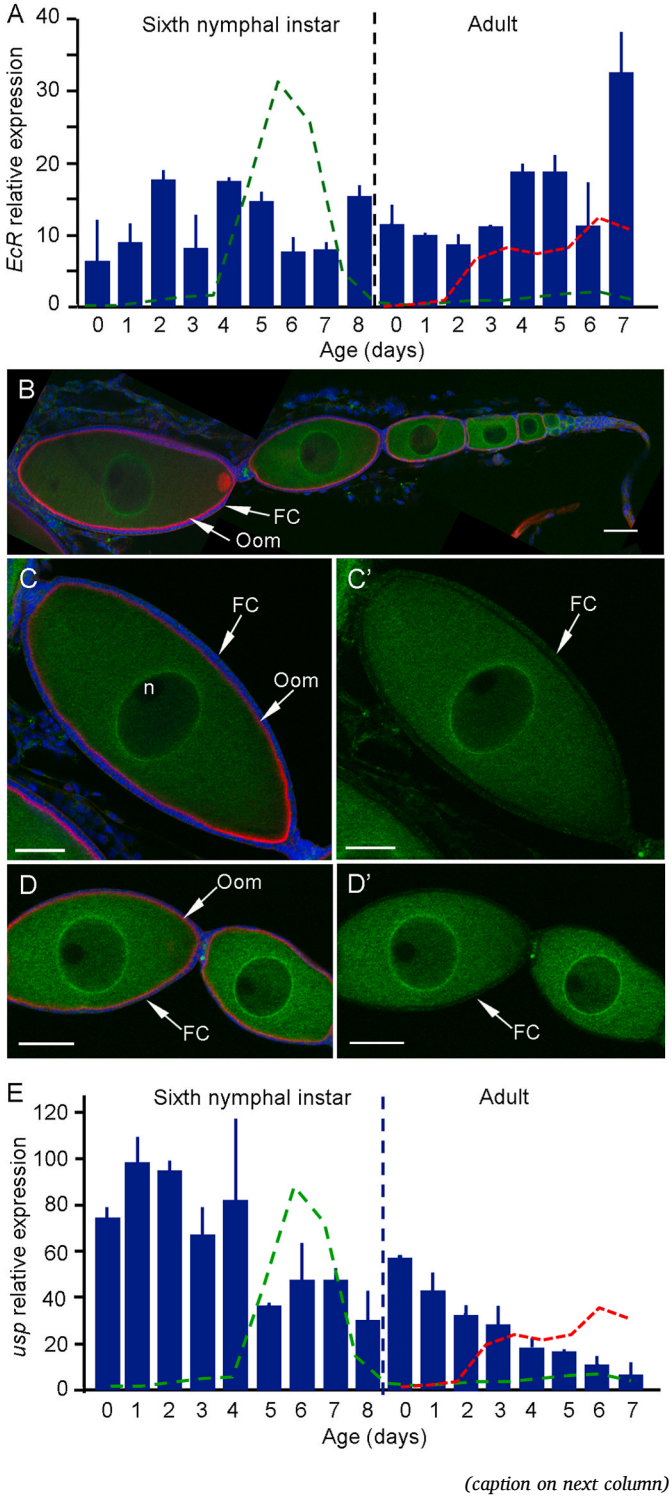

Fig. 1. *EcR and usp* in the ovaries of *Blattella germanica*. A. Expression pattern of *EcR* in ovaries, during the sixth (last) nymphal instar and the adult during the first gonadotropic cycle. **B.** Ovariole from a 6-day-old sixth instar nymph (N6D6). EcR labelling can be observed in all the ovarian follicles, concentrated around the nucleus. **C.** EcR labelling in the basal ovarian follicle. Labelling can be observed in the oocyte cytoplasm and in the oocyte nucleus, with a higher labelling concentration around the nuclear membrane. EcR labelling can also be detected in the follicular cells (**C′**). **D-D'**. Younger ovarian follicles showing the same distribution of EcR labelling. In these younger oocytes the signaling is more intense. DAPI (blue) was used for DNA staining and phalloidin-TRITC (red) was used to stain F-actin microfilaments. The terminal filament is shown towards the right. Scale bar: 50 μm. FC: Follicular cells. Oom: oocyte membrane. n: nucleolus. **E.** Expression pattern of *usp* in ovaries, during the sixth (last) nymphal instar and the adult during the first gonadotropic cycle. Data shown in A and E, represent copies of mRNA per 1000 copies of *actin-5c* and are expressed as the mean ± S.E.M. (n = 3–6). Profiles of ecdysteroid titres in the haemolymph (green dashed line) and ecdysteroid content in the ovaries (red dashed line) are also shown. The ecdysteroid data is from Cruz et al. (2003), Pascual et al. (1992) and Romañá et al. (1995).

Because USP is the co-receptor of 20E along with EcR, we also measured the expression of *usp* in the ovaries during the first gonadotrophic cycle. The results (Fig. 1E) show that the *usp* expression profile is different from that of *EcR*. More specifically, there were streaking differences in the adult stage, with *usp* transcript levels progressively decreasing, reaching the lowest values to just before oviposition (Fig. 1E). At this age, its expression was significantly reduced ($p = 0.044$) by 86.9%, compared with the expression levels in newly emerged last instar nymphs.

3.2. Effects of EcR depletion on ecdisteroidogenic and ecdysone signaling genes

To study the function of *EcR* in the ovary, ds*EcR* was injected into the abdomen of newly emerged sixth instar nymphs. As reported previously (Cruz et al., 2006), none of the ds*EcR*-treated insects (n = 23) completed the ecdysis. Conversely, all control specimens (n = 22) moulted correctly. Previous studies showed that circulating ecdysteroids were not detected in ds*EcR* treated insects (Cruz et al., 2006). Thus, we prepared a new batch of ds*EcR*-treated nymphs to measure the expression of *EcR*, as well as that of the ecdysteroidogenic genes *neverland (nvd)*, *phantom (phm)*, *shadow (sad)* and *shd*. Measurements were carried out in the prothoracic gland of 6-day-old dsPolyH (n = 6) and ds*EcR*-treated nymphs (n = 6), coinciding with the peak of ecdysteroids in the haemolymph (Fig. 2A).

The expression of *EcR* in the prothoracic gland decreased by 21% as average (Fig. 2A) in ds*EcR*-treated insects, although differences with respect to the controls were not statistically significant. However, expression of the ecdysteroidogenic genes was significantly reduced (Fig. 2B), with *nvd* showing the greatest reduction (97.65%, $p < 0.001$), followed by *phm* (58.99%, $p < 0.001$), and *sad* (69.46%, $p < 0.01$); *shd* expression was not detected in the prothoracic gland.

EcR expression was also measured in the ovaries from the 6-day-old dsPolyH- and ds*EcR*-treated nymphs, obtained in the aforementioned experiments. Unexpectedly, *EcR* expression was similar to that of controls (Fig. 2C). To evaluate if 20E signaling was prevented in the ovaries due to the ds*EcR* treatment, the expression of the ecdysone-dependent

(caption on next column)

genes *E75A, E78* and *HR3*, was also measured. The results (Fig. 2C) showed that the expression of all of them was significantly reduced, thereby indicating that the 20E signaling had been impaired.

To assess when *EcR* expression was reduced, transcript levels of *EcR* and *E75A* were measured in ovaries of last instar nymphs 2, 4, 6, and 8 days after the ds*EcR* treatment. *EcR* expression was 36.46% and 38.2%

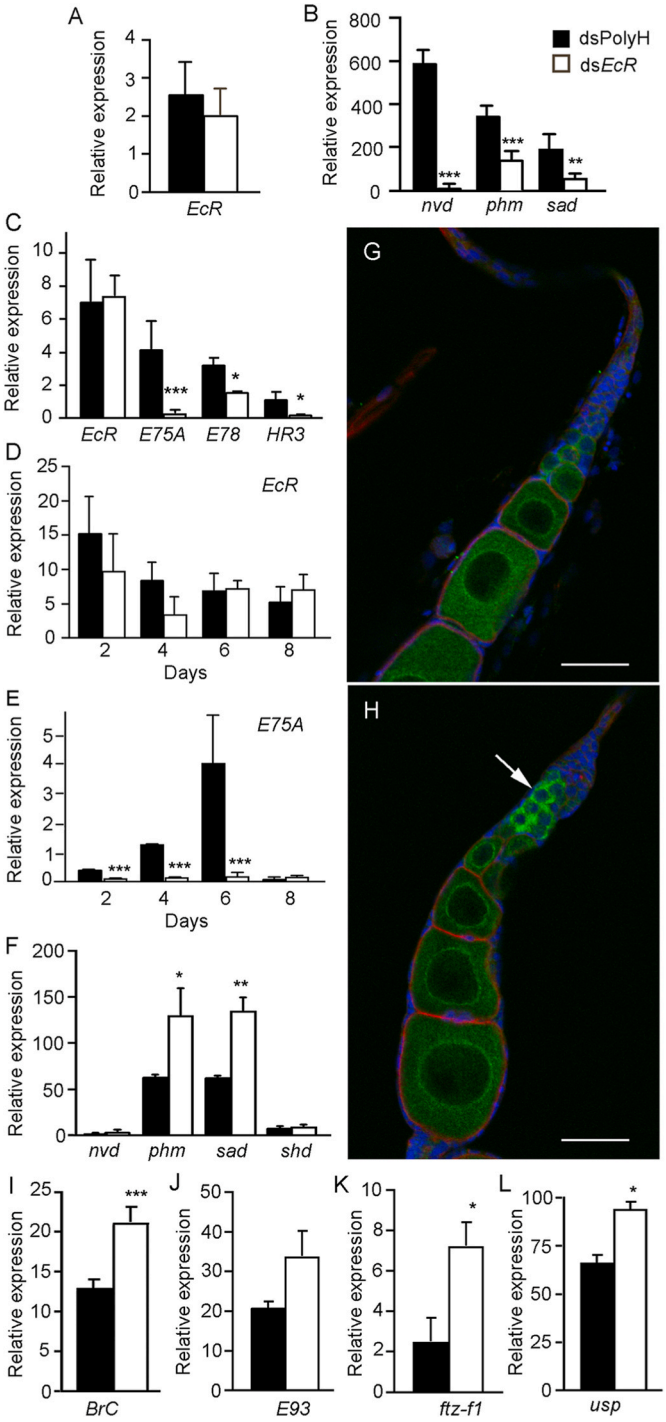

Fig. 2. *EcR* depletion in the prothoracic gland and ovaries of 6-day-old *Blattella germanica* sixth instar nymphs. A. Expression of *EcR* in the prothoracic gland of ds*EcR* and dsPolyH treated nymphs. **B.** Expression of *neverland (nvd), phantom (phm)* and *shadow (sad)* in the prothoracic gland of ds*EcR* and dsPolyH treated nymphs. **C.** Expression of *EcR, E75A, E78* and *HR3* in ovaries from dsPolyH- and ds*EcR*-treated nymphs. **D.** Expression of *EcR* in ovaries from 2-, 4-, 6- and 8-day-old, ds*EcR*-treated nymphs. **E.** Expression of *E75A* in ovaries of 2-, 4-, 6- and 8-day-old, ds*EcR*-treated nymphs. **F.** Expression of *nvd*, *phm*, *sad*, and *shd* in ovaries from 6-day-old sixth instar nymphs. **G.** Germarium from a dsPolyH-treated nymph showing strong EcR labelling in the cells at the bottom of the germarium and close to the vitellarium. **H.** Germarium from a ds*EcR*-treated nymph, EcR labelling in the germarium cells was increased (arrow), compared to dsPolyH-treated nymphs. **I-L.** Expression levels of *BrC* (I) *E93* (J), *ftz-f1* (K) and *usp* (L), in ovaries from dsPolyH and ds*EcR* treated N6D6 nymphs. qRT-PCR data (panels A–F and I-L) represent copies of mRNA per 1000 copies of *actin-5c* and are expressed as mean ± S.E.M. (n = 3–6). Asterisks indicate statistically significant differences at probability levels of $p < 0.05$ (*); $p < 0.01$ (**), and $p < 0.001$ (***). In panels G and H, DAPI (blue) was used for DNA staining and phalloidin-TRITC (red) was used to stain F-actin microfilaments. The terminal filament is towards the top of the panel. Scale bars: 50 μm.

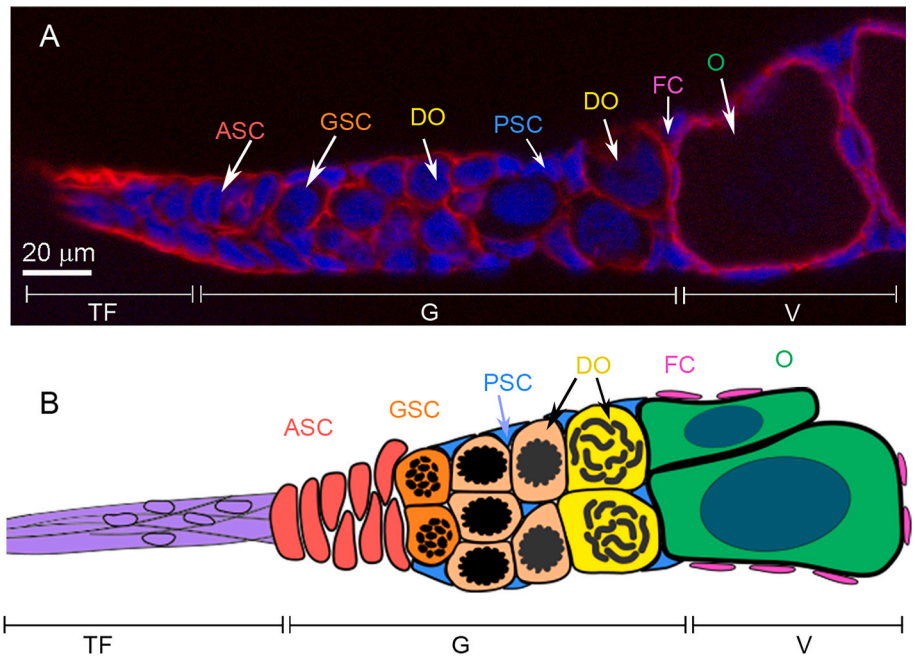

Fig. 3. The *Blattella germanica* germarium. A. Germarium from a 6-day-old sixth (last) nymphal instar (N6D6). **B.** Schematic representation of the germarium corresponding to a N6D6 nymph. The abbreviations in various colors indicate the different cell types identified. The germarium (G) is located between the terminal filament (TF) and the vitellarium (V). Within the germarium putative germinal stem cells (GSCs; orange) are in close contact with the apical somatic cells (ASC; red) and these give rise to the differentiating oocytes (DO; light orange and yellow), which show different stages of meiosis. Furthermore, peripheral somatic cells (PSC; blue) and follicular cells (FC; pink) that surround the early differentiated oocytes (O; green) could be identified. The latter two cell types conform the ovarian follicles and are located in the vitellarium region. In the image, nuclei are stained with DAPI (blue), and Phalloidin-TRITC (red) was used to stain F-actin microfilament. The terminal filament is shown towards the left.

reduced in 2- and 4-day-old nymphal ovaries, respectively, although differences compared to the controls were not statistically significant (Fig. 2D). Nonetheless, the expression of *E75A* was significantly ($p < 0.001$) reduced two days after the treatment with ds*EcR*, and this low *E75A* expression was maintained during the entire instar (Fig. 2E). We analyzed the presence of EcR immunolabelling in the ovarioles and, in comparison with controls (Fig. 2G), we detected an accumulation of EcR in the cells of the basal part of the germarium, at the transition with the vitellarium (Fig. 2H, arrow).

We presumed that even if the *EcR* expression was not markedly reduced in the ovary, the depletion of ecdysteroidogenic genes in the prothoracic gland would determine a reduction of produced and circulating ecdysteroids, and consequently an impairment of 20E signaling in the ovary. However, although the prothoracic gland is the main source of ecdysone during nymphal stages, ecdysteroidogenic genes are also expressed in ovaries from the last nymphal instar, suggesting that the ovaries also synthesize ecdysone during this stage (Ramos et al., 2020). Thus, we decided to measure the expression of *nvd*, *phm*, *sad* and *shd* in ovaries from 6-day-old last instar nymphs in dsPolyH and ds*EcR*-treated specimens. Again unexpectedly, *phm* and *sad* expression significantly increased ($p < 0.05$ and $p < 0.01$, respectively) in the ovaries of ds*EcR*-treated nymphs. However, the expression of *nvd* (the first enzyme in the ecdysone pathway) and *shd* (the last enzyme in the pathway), was not affected (Fig. 2F).

Taken together, the results suggest that some genes from the ecdysone pathway in the prothoracic gland and ovaries responded in opposing ways to the ds*EcR* treatment. In addition, the EcR labeling intensity in the germarium of ds*EcR*-treated nymphs led us to hypothesize that EcR plays a function in the germarium of panoistic ovaries.

Finally, we measured the expression levels of other 20E-related genes and found that the expression of *Broad-complex* (*BrC*), *fushi tarazu factor 1* (*ftz-f1*), and *usp* significantly increased in ovaries of last instar nymphs treated with ds*EcR* (Fig. 2I-L), while *E93* only shows a tendency to increase its expression. These results suggest that in ovaries of this stage, *EcR* can act as an activator of some genes (*E75A*) and as a repressor of others (*BrC*, *E93*, *ftz-f1*, and *usp*). Having these results, we wondered whether EcR in the adult ovary, when the prothoracic gland has degenerated, can exert the same function. Newly emerged adult females were treated with 1 μg of ds*EcR* or dsPolyH ($n = 6$), and we observed that any of the ds*EcR* treated females oviposited, and the basal ovarian follicles finally degenerated and started to be reabsorbed. In a new batch of experiments ($n = 3$) females were dissected on day seven coinciding with the process of choriogenesis in controls, and we measured de expression of 20E related genes in ovaries. *EcR* expression was significantly reduced by an 81.64%. In a similar way, *E75A* (97.59%), *usp* (49.94%), and *E93* (67.9%) were reduced (Fig. S1). The ecdysteroidogenic genes were also measured, *nvd* (37.8%), *spo* (74.55%), *phm* (46.23%) and *sha* (67.27%) showed a reduction in their expression. Only *shd* increase its expression levels with a fold change of 2 (Fig. S1).

3.3. The germarium of the panoistic ovary of *B. germanica*

We identified different cell types in the germarium from 6-day-old last instar nymphs (Fig. 3A and B). A series of flattened cells are present in the apical part of the germarium, just at the transition between the terminal filament and the germarium itself (Fig. 3A and B; red cells in B). Usually, these cells are distributed in intercalated pairs that remind the cap cells of *D. melanogaster*. In the panoistic ovary of the firebrat *T. domestica* (Tworzydlo et al., 2014) these are referred as apical somatic cells, and so we kept this nomenclature in *B. germanica* (Fig. 3A and B). Again, by analogy with the germarium of *D. melanogaster*, the putative germinal stem cells are in close contact with the apical somatic cells (ASC; Fig. 3A and B). In the meroistic polytrophic ovary of *D. melanogaster*, the terminal filament and cap cells constitute the niche, and project Dpp signaling to the germinal stem cells, thereby maintaining their totipotency.

Again in *D. melanogaster*, the germinal stem cells undergo asymmetric divisions in which one daughter cell remains in the niche as a stem cell, while the other starts differentiating becoming an oocyte and the accompanying nurse cells (Gancz et al., 2011). In species with panoistic ovaries, two possibilities have been reported (Büning, 1994). One is that all germinal cells give oocytes, like in *Locusta migratoria*, which does not have germaria, whereas in other species the division of the stem cell give two cells by differentiated mitosis, one of them remains as a stem cell, while the other differentiates into an oocyte (Büning, 1994). In the germarium of *B. germanica*, a number of early oocytes in an intermediate differentiation stage can be observed just after the germinal stem cells (Fig. 3B, cells in pale orange). These initial not-fully-differentiated oocytes contain DNA packed into small ball-like

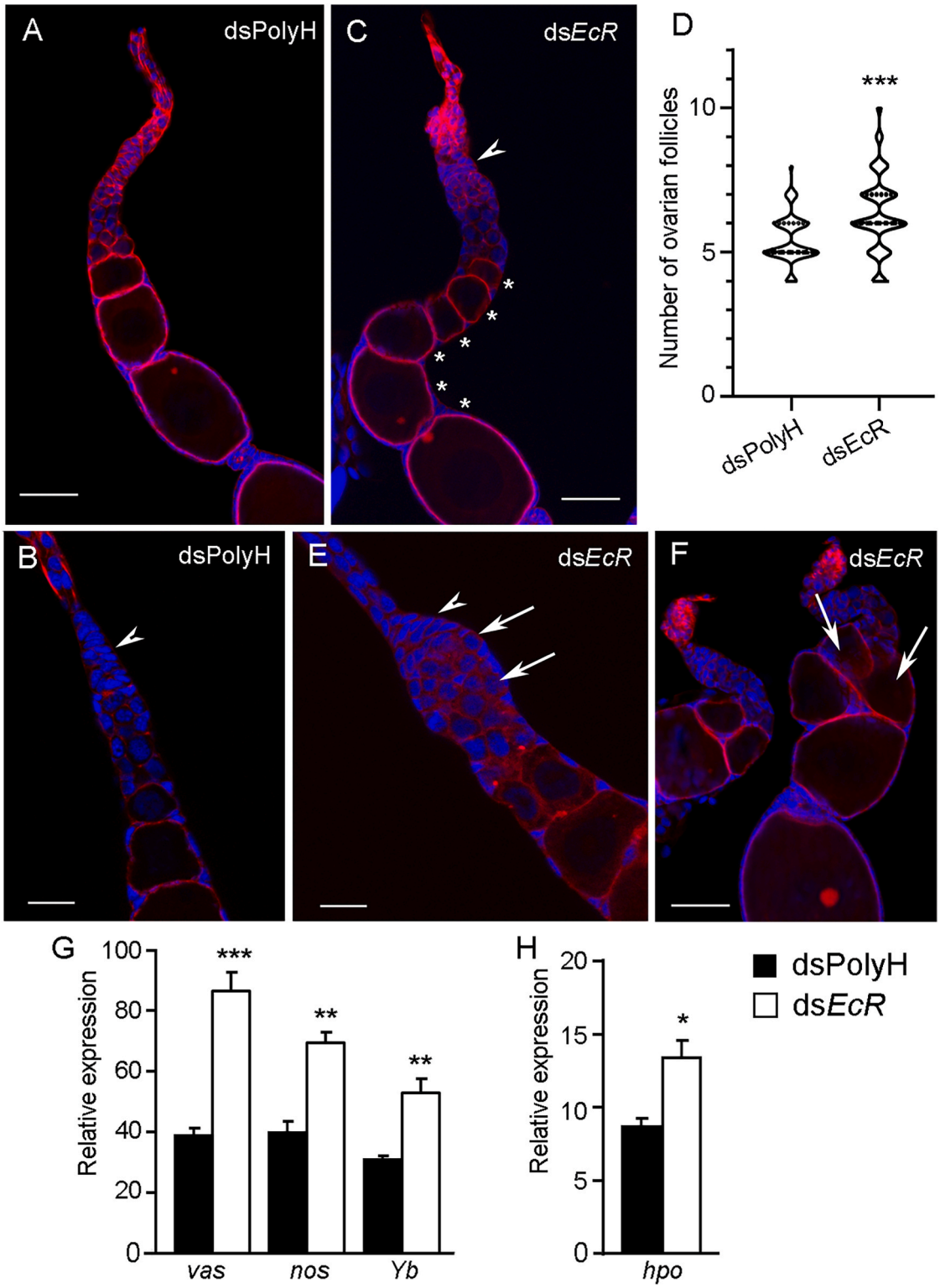

Fig. 4. ***EcR*** **depletion on cell proliferation and ecdysone regulated genes in** ***Blattella germanica*****.** Ovariole (**A**) and germarium (**B**) from a six-day-old sixth instar (N6D6) nymph treated with dsPolyH. The arrowhead in B indicates apical somatic cells. **C, E** and **F:** Ovarioles and germaria representatives of the three phenotypes observed in ds*EcR*-treated N6D6 nymphs. In C, the arrowhead indicates the swollen germarium. In E, the arrows indicate oocytes in an undetermined stage of differentiation, while the arrowhead indicates the apical somatic cells. In F, arrows indicate the first differentiated ovarian follicles in the vitellarium. **D**: Number of differentiated ovarian follicles in N6D6 ovarioles from dsPolyH and ds*EcR* treated nymphs. We quantified all differentiated ovarian follicles excluding the basal one in 127 ovarioles of 24 dsPolyH-treated nymphs, and 133 ovarioles from 19 ds*EcR*-treated nymphs. In all the images, nuclei were stained with DAPI (blue) and F-actin microfilament with phalloidin-TRITC (red). The scale bar in A, C and F represents 50 μm, and in B and E 20 μm. In the images, the terminal filament is shown towards the top. **G.** Expression levels of *vasa* (*vas*), *nanos* (*nos*), and *fs(1)Yb* (*Yb*), in dsPolyH and ds*EcR*-treated ovaries from N6D6 nymphs. **H.** Expression levels *hippo* (*hpo*) in dsPolyH and ds*EcR*-treated ovaries from N6D6 nymphs. Data represent copies of mRNA per 1000 copies of *actin-5c* and are expressed as mean ± S.E.M. (n = 3–6). Asterisks represent statistically significant differences at $p < 0.04$ (*); $p < 0.001$ (**), and $p < 0.0001$ (***).

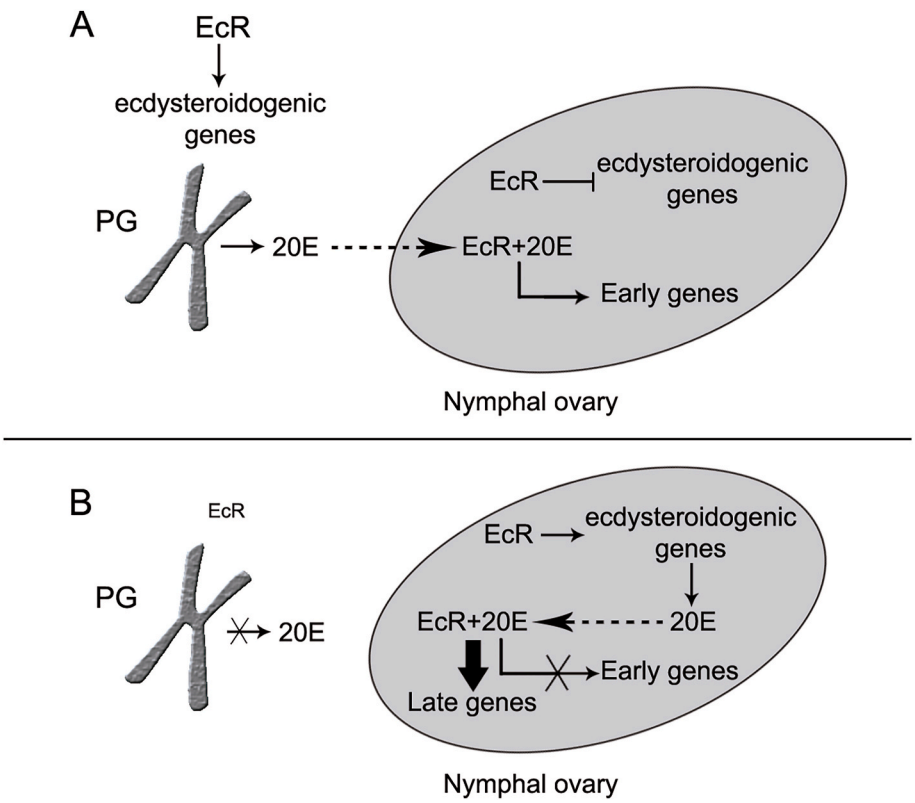

Fig. 5. The modes of action of EcR in the prothoracic gland and in the ovary in the last nymphal instar of *Blattella germanica*. In the prothoracic gland (PG) EcR promotes ecdysone synthesis by activating the expression of ecdysteroidogenic genes, whereas in the ovary, EcR appears to repress the activity of these genes. (A) When there is 20E circulating in the haemolymph that comes from the PG, EcR transduces the hormonal signal activating early genes of the Ashburner cascade, such as *E75A*. (B) When the only source of 20E is the nymphal ovary, EcR appears to function as a transcription factor repressing other 20E-associated genes, like *BrC* or *ftz-f1*.

heterochromatin aggregations. Immediately next to these formations, a number of early meiotic oocytes are observed with DNA starting to condense into chromosomes (DO; Fig. 3A and B). In between these early meiotic oocytes, and surrounding them, somatic triangular cells could be seen which resembled the escort cells from *D. melanogaster*. Using *T. domestica* terminology as a reference (Tworzydlo et al., 2014), here we refer to them as peripheral somatic cells (PSC; Fig. 3A and B).

3.4. Effects of EcR depletion on the germarium

We observed 133 ovarioles from 19 ds*EcR*-treated nymphs, and 127 ovarioles from 24 dsPolyH-treated nymphs. In all the ovarioles from ds*EcR*-treated nymphs we detected changes related with cell proliferation at different levels. In 74% of these ovarioles from ds*EcR*-treated nymphs the germarium appear to be swollen (39.54 ± 1.76 μm; $p < 0.0001$; Fig. 4C and E) compared to those from dsPolyH-treated nymphs (23.14 ± 1.19 μm; Fig. 4A and B). This suggests that an increase in cell proliferation and/or differentiation in the germarium was produced. Nevertheless, early oocytes were not fully differentiated and were at an intermediate stage between undifferentiated germinal stem cells and differentiated oocytes (Fig. 4E, arrows). Moreover, the usual organization of cells found in the germarium of 6-day-old last instar nymphs was perturbed (compare Fig. 4B and E). Different cell types were intermingled in the germarium of ds*EcR*-treated nymphs (Fig. 4E). The apical somatic cells acquired a new arrangement (Fig. 4C and E, arrowhead) and they were not as flat as in the control ovaries (Fig. 4B, arrowhead). Instead of being located in a linear array of intercalated pairs, the apical somatic cells formed an Λ-shape that hugged the germinal stem cells (Fig. 4E, arrowhead and arrows). In addition, there was an increase in the number of germarium cells in 58% of the ovarioles from ds*EcR*-treated nymphs (Fig. 4C and F). Moreover, the terminal filament in these ovarioles appeared to be thicker and had more F-actin filaments than in the controls (Fig. 4A and B).

In addition to the swollen germarium already described, a significant group of the ds*EcR*-treated nymphs showed a higher number ($p < 0.0001$) of differentiated ovarian follicles in the vitellarium when compared to the controls (Fig. 4C asterisks, and Fig. 4D). This was reminiscent of the phenotype obtained after injecting 20E into newly emerged last instar nymphs (Ramos et al., 2020). In these 20E-injected females, the number of ovarian follicles in the vitellarium also increases, even though the cells were the same as in the control ovaries, albeit with a very thin germarium (Ramos et al., 2020). Moreover, the cells in the germarium appear disorganized in 20% of the ovarioles from dsEcR-treated nymphs, although their size did not differ from the controls. Instead, in these individuals the first differentiated ovarian follicles in the vitellarium appeared bigger (Fig. 4F, arrows) than those in the ovaries from controls (Fig. 4A).

3.5. Effects of EcR depletion on the expression of genes of different pathways in the ovary

In most ds*EcR*-treated nymphs, the germarium appeared to be disorganized and larger. However, like the females treated with 20E (Ramos et al., 2020), the vitellarium generally contained more differentiated ovarian follicles. All of our observations indicated that, as occurs in meroistic ovaries, the ecdysone contributes to niche organisation and maintenance of correct cell proliferation and differentiation in panoistic ovaries. Thus, we measured the expression of *vasa* (*vas*) as a germ cell marker, as well as of *nanos* (*nos*) and *fs(1)Yb* (*Yb*), two genes that are crucial in the modulation of germinal and somatic stem cell proliferation in *D. melanogaster* (King et al., 2001; Wang and Lin, 2004). The expression of these three genes increased significantly in ds*EcR*-treated insects ($p < 0.008$), thereby suggesting that the proliferation of germinal and somatic cells had increased (Fig. 4G). We also measured *hippo* (*hpo*) expression, as a gene that contributes to maintain the correct proportion of germinal and somatic cells in insect ovaries (Sarikaya and Extavour, 2015). In ds*EcR*-treated females, *hpo* expression also significantly increased in comparison with the controls (Fig. 4B, $p = 0.05$).

4. Discussion

The role of ecdysone in insect oogenesis has been thoroughly studied in model species with meroistic ovaries such as *D. melanogaster* and *B. mori* (see Bellés and Piulachs, 2015; Hayashi et al., 2020; Takaki et al., 2020). However, the function of ecdysone in panoistic ovaries is still poorly understood. In the present work, we studied the involvement of ecdysone signaling in oogenesis in the cockroach *B. germanica* by depleting *EcR* expression. Treatment with ds*EcR* reduced the expression of ecdysteroidogenic genes in the prothoracic gland in the last instar nymphs, and prevented the adult molt. These results are consistent with the depletion of ecdysteroid levels in the haemolymph observed after *EcR* depletion (Cruz et al., 2006).

Conversely, there was an increase in the expression of ecdysteroidogenic genes in the ovaries from ds*EcR*-treated nymphs. These results indicate that a number of genes from the ecdysone pathway in the prothoracic gland and ovaries responded to the ds*EcR* treatment in opposite ways. Our observations suggest that the ovary appears to enhance 20E synthesis as a response to the reduction of circulating ecdysteroids originating in the prothoracic gland. This sort of compensatory effect between ovaries and the prothoracic gland in terms of the expression of ecdysteroidogenic genes, does not occur in the locust *Schistocerca gregaria*, whose ovaries are also panoistic. In this species, although ds*EcR* treatment prevents ovarian maturation and oviposition, the transcript levels of the ecdysteroidogenic genes in the ovary are unaffected (Lenaerts et al., 2019).

In ds*EcR*-treated nymphs of *B. germanica*, the upregulation of ecdysteroidogenic genes resulted in an increase in the number of differentiated ovarian follicles in the ovariole. This result appeared to be associated with the accumulation of EcR labelling observed in early oocytes in the germarium. The increase in differentiated ovarian follicles is reminiscent of the results obtained after applying exogenous 20E to last instar *B. germanica* nymphs (Ramos et al., 2020), where this treatment triggered a significant upregulation of *E75* expression, thus suggesting that the 20E activated the early genes in the ecdysone cascade. In the present experiments, ds*EcR* treatment triggered a downregulation in *E75* expression in nymphal ovaries, which was maintained thorough the instar. This depletion could be the result of the absence in the haemolymph of 20E from the prothoracic gland, suggesting that the ecdysone produced by nymphal ovaries is not transduced through *E75A*. However, the ds*EcR* treatment, independently affects other 20E-associated genes including *BrC*, *usp*, *ftz-f1* and *E93* that appear upregulated. These results can be explained by considering the multifunctional action of EcR, which can act as activator or repressor depending on the physiological inputs associated with hormonal changes, tissue specificity or developmental stages (Dobens et al., 1991; Uyehara and McKay, 2019). In this sense, our results are consistent with the data described in the red flour beetle *T. castaneum*, in which *E75* expression is not induced by the ecdysone synthesized in the ovary (Takaki et al., 2020). Our findings also agree with those reported for *D. melanogaster* suggesting that, in the absence of 20E, *EcR* could play a role different from that of hormonal receptor, depending on the tissue and temporal line (Uyehara et al., 2022; Uyehara and McKay, 2019).

The most notable and frequent phenotype observed in the ovaries of ds*EcR*-treated nymphs was the increase of cell proliferation and incomplete differentiation, resulting in a swollen germarium. This phenotype reminds the results obtained for *D. melanogaster* (König et al., 2011; Kozlova and Thummel, 2002) after preventing ecdysone biosynthesis and depleting the expression of dominant-negative mutants for *EcR*, which resulted in a larger germarium. These researchers suggested that the increase in germarium size was because of a delay in the differentiation of germinal stem cells caused by a differential adhesion between germinal stem cells and mutant somatic cells (König and Shcherbata, 2015). Further work should be necessary to clarify whether these explanations can be applied to the panoistic ovary of *B. germanica*.

In any case, our results clearly indicate that EcR has differentiated modes of action in the prothoracic gland and ovary in the last nymphal instar of *B. germanica* (Fig. 5) While in the prothoracic gland EcR promotes ecdysone synthesis by activating the expression of ecdysteroidogenic genes, in the ovary EcR appears to repress the activity of these genes (Fig. 5A). In addition, we found that the nymphal ovary responds differently to ecdysone depending on the hormonal source. Thus, when there is 20E circulating in the haemolymph and coming from the prothoracic gland, EcR transduces the hormonal signal activating early genes in the canonical signaling cascade (in the sense of Ashburner, 1980) such as *E75A* (Fig. 5A). However, when the only source of 20E is the nymphal ovary, EcR appears to function as a transcription factor repressing other 20E-associated genes, like *BrC* or *ftz-f1* (Fig. 5B). The mechanism of action for this bimodal effect on gene expression, both as an activator and repressor, may lie in the EcR activities as regulator of enhancer activity, as shown in *D. melanogaster* (Dobens et al., 1991; Uyehara et al., 2022).

Acknowledgments

We thank the financial support through the projects PID2021-122316OB-I00 from the MCIN/AEI/10.13039/501100011033 and by ERDF a way of making Europe, by the “European Union”. The funders had no role in the design of the study, data collection or analysis, the decision to publish, or in the preparation of the manuscript. Thanks, are also due to Xavier Bellés for critically reading a previous version of the manuscript.

Appendix A. Supplementary data

Supplementary data to this article can be found online at https://doi.org/10.1016/j.ibmb.2023.103935.

References

Ashburner, M., 1980. Chromosomal action of ecdysone. Nature 285, 435–436.
Baldini, F., Gabrieli, P., South, A., Valim, C., Mancini, F., Catteruccia, F., 2013. The interaction between a sexually transferred steroid hormone and a female protein regulates oogenesis in the malaria mosquito *Anopheles gambiae*. PLoS Biol. 11, e1001695 https://doi.org/10.1371/journal.pbio.1001695.
Behrens, W., Hoffmann, K., 1983. Effects of exogenous ecdysteroids on reproduction in crickets, *Gryllus bimaculatus*. Int. J. Invertebr. Reprod. 6, 149–159. https://doi.org/10.1080/01651269.1983.10510037.
Bellés, X., Cassier, P., Cerdá, X., Pascual, N., André, M., Rossó, Y., Piulachs, M.D., 1993. Induction of choriogenesis by 20-hydroxyecdysone in the German cockroach. Tissue Cell 25 (2), 195–204.
Bellés, X., Piulachs, M.D., 2015. Ecdysone signalling and ovarian development in insects: from stem cells to ovarian follicle formation. Biochim. Biophys. Acta 1849, 181–186. https://doi.org/10.1016/j.bbagrm.2014.05.025.
Benrabaa, S., Orchard, I., Lange, A.B., 2022. The role of ecdysteroid in the regulation of ovarian growth and oocyte maturation in *Rhodnius prolixus*, a vector of Chagas disease. J. Exp. Biol. 225 https://doi.org/10.1242/jeb.244830 jeb244830.
Cruz, J., Martín, D., Pascual, N., Maestro, J.L., Piulachs, M.D., Bellés, X., 2003. Quantity does matter. Juvenile hormone and the onset of vitellogenesis in the German cockroach. Insect Biochem. Mol. Biol. 33, 1219–1225. https://doi.org/10.1016/j.ibmb.2003.06.004.
Büning, J., 1994. The Insect Ovary : Ultrastructure, Previtellogenic Growth and Evolution. Springer, Netherlands.
Cruz, J., Mané-Padrós, D., Bellés, X., Martín, D., 2006. Functions of the ecdysone receptor isoform-A in the hemimetabolous insect *Blattella germanica* revealed by systemic RNAi in vivo. Dev. Biol. 297, 158–171. https://doi.org/10.1016/j.ydbio.2006.06.048.
Dobens, L., Rudolph, K., Berger, E.M., 1991. Ecdysterone regulatory elements function as both transcriptional activators and repressors. Mol. Cell Biol. 4, 1846–1853. https://doi.org/10.1128/mcb.11.4.1846-1853.1991.
Drummond-Barbosa, D., 2019. Local and physiological control of germline stem cell. Genetics 213, 9–26. https://doi.org/10.1534/genetics.119.300234.
Finger, D.S., Whitehead, K.M., Phipps, D.N., Ables, E.T., 2021. Nuclear receptors linking physiology and germline stem cells in Drosophila. In: Litwack, G. (Ed.), Vitamins and Hormones. Elsevier Inc, pp. 327–362. https://doi.org/10.1016/bs.vh.2020.12.008.
Gancz, D., Lengil, T., Gilboa, L., 2011. Coordinated regulation of niche and stem cell precursors by hormonal signaling. PLoS Biol. 9, e1001202 https://doi.org/10.1371/journal.pbio.1001202.
Hayashi, Y., Yoshinari, Y., Kobayashi, S., Niwa, R., 2020. The regulation of *Drosophila* ovarian stem cell niches by signaling crosstalk. Curr. Opin. Insect Sci. 37, 23–29. https://doi.org/10.1016/j.cois.2019.10.006.

Hsu, H.J., Bahader, M., Lai, C.M., 2019. Molecular control of the female germline stem cell niche size in *Drosophila*. Cell. Mol. Life Sci. 76, 4309. https://doi.org/10.1007/s00018-019-03223-0.

Hult, E., Huang, J., Marchal, E., Lam, J., Tobe, S., 2015. RXR/USP and EcR are critical for the regulation of reproduction and the control of JH biosynthesis in *Diploptera punctata*. J. Insect Physiol. 80, 48–60. https://doi.org/10.1016/j.jinsphys.2015.04.006.

Irles, P., Piulachs, M.D., 2014. Unlike in Drosophila Meroistic Ovaries, hippo represses notch in *Blattella germanica* Panoistic ovaries, triggering the mitosis-endocycle switch in the follicular cells. PLoS One 9, e113850. https://doi.org/10.1371/journal.pone.0113850.

Irles, P., Belles, X., Piulachs, M.D., 2009. Identifying genes related to choriogenesis in insect panoistic ovaries by Suppression Subtractive Hybridization. BMC Genom. 10, 206. https://doi.org/10.1186/1471-2164-10-206.

King, D.S., Bollenbacher, W.E., Borst, D.W., Vedeckis, W.V., O'Connor, J.D., Ittycheriah, P.I., Gilbert, L.I., 1974. The secretion of a-ecdysone by the prothoracic glands of *Manduca sexta* in vitro. Proc. Natl. Acad. Sci. USA 71, 793–796. https://doi.org/10.1073/pnas.71.3.793.

King, F.J., Szakmary, A., Cox, D.N., Lin, H., 2001. *Yb* modulates the divisions of both germline and somatic stem cells through piwi- and hh-mediated mechanisms in the *Drosophila* ovary. Mol. Cell. 7, 497–508. https://doi.org/10.1016/S1097-2765(01)00197-6.

Klowden, M.J., 2007. Physiological Systems in Insects. Academic Press.

König, A., Shcherbata, H., 2015. Soma influences GSC progeny differentiation via the cell adhesion-mediated steroid-let-7-Wingless signaling cascade that regulates chromatin dynamics. Biol. Open 4, 285–300. https://doi.org/10.1242/bio.201410553.

König, A., Yatsenko, A.S., Weiss, M., Shcherbata, H.R., 2011. Ecdysteroids affect *Drosophila* ovarian stem cell niche formation and early germline differentiation. EMBO J. 30, 1549–1562. https://doi.org/10.1038/emboj.2011.73.

Kozlova, T., Thummel, C.S., 2002. Spatial patterns of ecdysteroid receptor activation during the onset of *Drosophila metamorphosis*. Development 129, 1739–1750. https://doi.org/10.1242/dev.129.7.1739.

Lenaerts, C., Marchal, E., Peeters, P., Vanden Broeck, J., 2019. The ecdysone receptor complex is essential for the reproductive success in the female desert locust, *Schistocerca gregaria*. Sci. Rep. 9, 1–12. https://doi.org/10.1371/journal.pone.0046109.

Livak, K.J., Schmittgen, T.D., 2001. Analysis of relative gene expression data using real-time quantitative PCR and the 2-ΔΔCT method. Methods 25 (4), 402–408. https://doi.org/10.1006/meth.2001.1262.

Maestro, O., Cruz, J., Pascual, N., Martín, D., Belles, X., 2005. Differential expression of two RXR/ultraspiracle isoforms during the life cycle of the hemimetabolous insect *Blattella germanica* (Dictyoptera, Blattellidae). Mol. Cell. Endocrinol. 1–2, 27–37. https://doi.org/10.1016/j.mce.2005.04.004.

Nation, J.L., 2008. Insect Physiology and Biochemistry. Taylor & Francis Group. https://doi.org/10.1201/9781420061789.

Parthasarathy, R., Sheng, Z., Sun, Z., Palli, S., 2010. Ecdysteroid regulation of ovarian growth and oocyte maturation in the red flour beetle, *Tribolium castaneum*. Insect Biochem. Mol. Biol. 40, 429–439. https://doi.org/10.1016/j.ibmb.2010.04.002.

Pascual, N., Cerdá, X., Benito, B., Tomás, J., Piulachs, M.D., Bellés, X., 1992. Ovarian ecdysteroid levels and basal oöcyte development during maturation in the cockroach *Blattella germanica* (L.). J. Insect Physiol. 38, 339–348. https://doi.org/10.1016/0022-1910(92)90058-L.

Pritsch, M., Büning, J., 1989. Germ cell cluster in the panoistic ovary of Thysanoptera (Insecta). Zoomorphology 108, 309–313. https://doi.org/10.1007/BF00312163.

Ramos, S., Chelemen, F., Pagone, V., Elshaer, N., Irles, P., Piulachs, M.D., 2020. Eyes absent in the cockroach panoistic ovaries regulates proliferation and differentiation through ecdysone signalling. Insect Biochem. Mol. Biol. 123, 103407 https://doi.org/10.1016/j.ibmb.2020.103407.

Robinson, R., 2013. His hormone, her oogenesis: how male malaria mosquitoes trigger female egg development. e1001694 PLoS Biol. https://doi.org/10.1371/journal.pbio.1001694.

Romañá, I., Pascual, N., Bellés, X., 1995. The ovary is a source of circulating ecdysteroids in *Blattella germanica* (Dictyoptera: blattellidae). Eur. J. Entomol. 93, 93–103.

Rozen, S., Skaletsky, H., 2000. Primer3 on the WWW for general users and for biologist programmers. Methods Mol. Biol. 132, 365–386. https://doi.org/10.1385/1-59259-192-2:365.

Sarikaya, D.P., Extavour, C.G., 2015. The hippo pathway regulates homeostatic growth of stem cell niche precursors in the *Drosophila* ovary. PLoS Genet. 11, e1004962 https://doi.org/10.1371/journal.pgen.1004962.

Swevers, L., 2019. An update on ecdysone signaling during insect oogenesis. Curr. Opin. Insect Sci. 31, 8–13. https://doi.org/10.1016/j.cois.2018.07.003.

Swevers, L., Iatrou, K., 2009. Ecdysteroids and ecdysteroid signaling pathways during insect oogenesis. Ecdysone Struct. Funct. 127–164. https://doi.org/10.1007/978-1-4020-9112-4_5.

Taddei, C., C, M., Maurizii, M., Scali, V., 1992. The germarium of panoistic ovarioles of *Bacillus rossius* (Insecta phasmatodea): larval differentiation. Invertebr. Reprod. Dev. 21, 47–56. https://doi.org/10.1080/07924259.1992.9672219.

Takaki, K., Hazama, K., Yazaki, M., Kotani, E., Kaneko, Y., 2020. Maturation of telotrophic ovary accompanied with ecdysteroidogenic activity and contrastive decrease in ecdysteroids in the whole body of red flour beetle, *Tribolium castaneum* (Coleoptera: tenebrionidae). Appl. Entomol. Zool. 55, 299–308. https://doi.org/10.1007/s13355-020-00682-x.

Tworzydlo, W., Kisiel, E., Kankowska, W., Bilinski, S., 2014. Morphology and ultrastructure of the germarium in panoistic ovarioles of a basal "apterygotous" insect, *Thermobia domestica*. Zoology 117, 200–206. https://doi.org/10.1016/j.zool.2014.01.002.

Uyehara, C., McKay, D., 2019. Direct and widespread role for the nuclear receptor EcR in mediating the response to ecdysone in *Drosophila*. Proc. Natl. Acad. Sci. USA 116, 9893–9902. https://doi.org/10.1073/pnas.1900343116.

Uyehara, C., Leatham-Jensen, M., McKay, D.J., 2022. Opportunistic binding of EcR to open chromatin drives tissue-specific developmental responses. Proc. Natl. Acad. Sci. USA 119, 1–12. https://doi.org/10.1073/pnas.2208935119.

Wang, Z., Lin, H., 2004. Nanos maintains germline stem cell self-renewal by preventing differentiation. Science 303. https://doi.org/10.1126/science.1093983, 2016–2019.

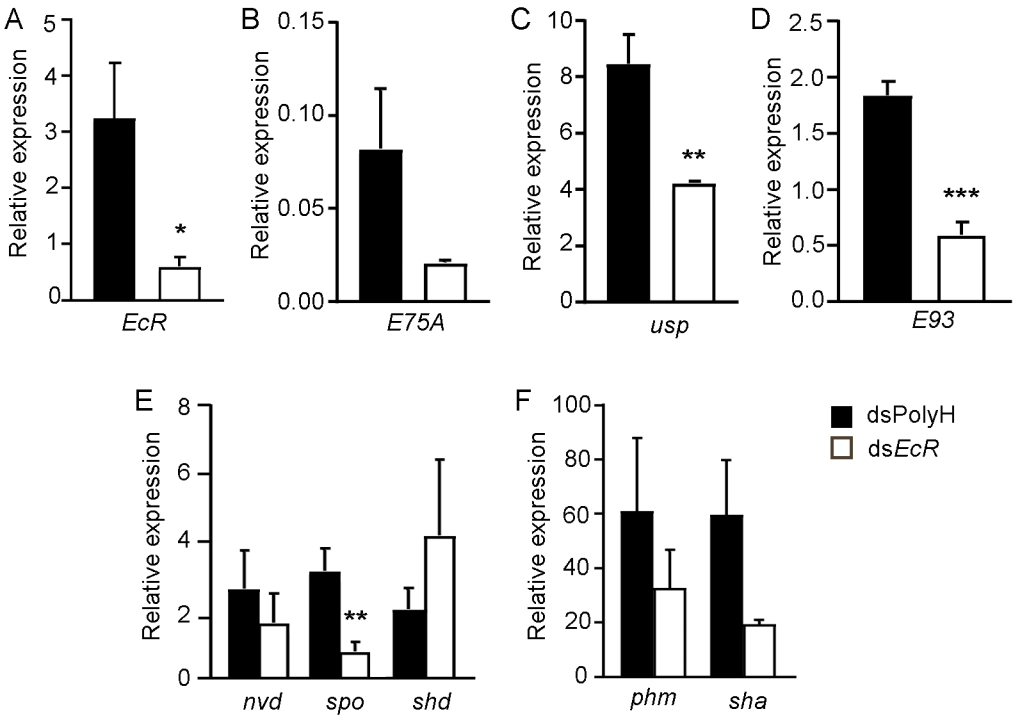

Figure S1. Effects of *EcR* depletion on the expression of different genes in the ovaries of 7-day-old adults of *Blattella germanica*. Newly emerged females were treated with 1 µg of ds*EcR* or dsPolyH (control), and dissected seven days later. Expression levels of *EcR* (A), *E75A* (B), *usp* (C), *E93* (D) and the ecdysteroidogenic genes *nvd*, *spo*, and *shd* (E) and *phm* and *sha* (F). qRT-PCR data are represented as copies of mRNA per 1000 copies of *actin-5c*, and are expressed as mean ± S.E.M. (n = 3 - 6). Asterisks indicate statistically significant differences at probability levels of $p < 0.05$ (*); $p < 0.03$ (**), and $p < 0.001$ (***).